Int. J. Heat Mass Transfer. Vol. 33, No. 1, pp. 163–173, 1990
Printed in Great Britain

0017–9310/90 $3.00 + 0.00

Unsteady heat and mass transfer with phase change in porous slabs: analytical solutions and experimental results

ANDREW P. SHAPIRO and SHAHRYAR MOTAKEF
Department of Mechanical Engineering, Massachusetts Institute of Technology, Cambridge, MA 02139, U.S.A.

(*Received* 23 *January* 1989 *and in final form* 2 *May* 1989)

Abstract—Unsteady one-dimensional heat and mass transfer with phase change in a porous slab is analytically investigated. It is shown that for a large class of problems the rate of motion of the wet zone can be decoupled from the transient change in the temperature and species fields, and the unsteady process can be reduced to that of quasi-steady fields in time-dependant domains. Analytical results are presented for mobile and immobile condensates. Reasonable agreement between the analytical solutions and experimental data is obtained.

1. INTRODUCTION

CURRENT interest in simultaneous heat and mass transfer with phase change in porous media stem from a spectrum of applications ranging from drying technology to design of energy efficient buildings. An area which has received considerable attention is related to the genesis of liquid water in open pore insulations and its effect on heat transfer through the building shell. In general, the source of liquid water in insulations can be related to water leakage or vapor condensation in the insulation package. In both instances the dynamics of heat and mass transfer in partially wet porous media is of significant importance to design of insulation packages and construction technology.

Simultaneous heat and mass transfer has been extensively studied for various systems [1–4]. These studies have been recently extended to condensation and liquid diffusion in open pore insulations [5–8]. Moisture migration in the presence of temperature gradients has been analyzed by Eckert and co-workers [5, 6] and Huang [7]. Condensation in insulations was first rigorously studied by Ogniewicz and Tien [8], where the coupling between temperature and concentration of condensing vapor was taken into account. Vafai and co-workers [9, 10] have recently obtained numerical solutions to one- and two-dimensional coupled transport equations. Experimental investigations of condensation in porous media, in contrast to modelling studies, have been relatively limited [13–17]. Whereas sophisticated models have been employed for solution of equations governing condensation in porous media, comparison of modelling results with experimental data have been scarcely reported.

In a previous publication [18], one-dimensional transport of heat and mass with phase change in a porous slab was studied, and analytical solutions for two limiting regimes of condensate diffusivity were obtained. In this work, the analysis is extended to unsteady transport processes. In the following the formalism for analytical solution of a large class of transient problems is presented, and the obtained results are compared with experimental results of the authors [17] and Thomas *et al.* [16].

2. ANALYSIS

Unsteady diffusion of heat, vapor and liquid is considered in a one-dimensional porous slab of thickness L_T, Fig. 1, with temperature and vapor concentration boundary conditions (T_I, C_I) and (T_{II}, C_{II}). Moisture, with an initial liquid content (by volume) distribution of $\theta(z)$, is assumed to occupy a single continuous zone (the 'wet zone') in the slab with boundaries at $z = L_0$ and L_1. The unsteady process starts from a set of initial temperature, vapor concentration and liquid (condensate) content distributions and boundary con-

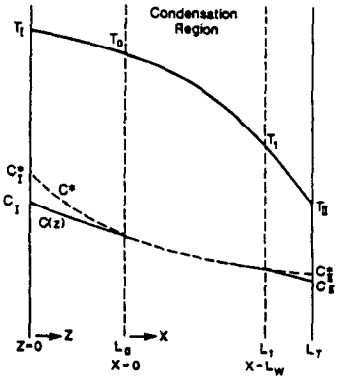

FIG. 1. Temperature and vapor concentration in a one-dimensional slab with a condensation region.

NOMENCLATURE

C	vapor concentration
C^*	saturation vapor concentration
C_r^*	$C^*(T_r)$
c	specific heat
D_{lm}	mean liquid diffusivity
$D_{l,v}$	diffusivity of liquid and vapor, respectively
h_{fg}	latent heat of condensation
$J_{l,v}$	liquid and vapor mass flux, respectively
k	thermal conductivity
L_T	total length of the slab
L_0	location of the warm boundary of the condensation region
L_1	location of the cold boundary of the condensation region
Le	Lewis number
T_r	reference temperature, $(T_I+T_{II})/2$
T_r'	reference temperature, $(T_0+T_1)/2$
t	time
x	length of scale in the condensation region
z	length scale in the slab.

Greek symbols

β	non-dimensional temperature drop, $(T_I+T_{II})/T_r$
β'	non-dimensional temperature drop, $(T_0-T_1)/T_r'$
Γ	volumetric condensation rate, $(Le\,\beta'/\Omega')(\lambda'^2/2)(\exp(\lambda' x)/\exp(\lambda')-1)$
γ	h_{fg}/RT_r
η	dimensionless temperature, $(T-T_r)/(T_I-T_{II})$
η'	dimensionless temperature, $(T-T_r)/(T_0-T_1)$
θ	liquid content
θ_c	critical liquid content
λ'	latent heat transport coefficient, $2\gamma'^2\beta'\Omega'/Le+\gamma'\omega'$
ρ	density
Φ	$\gamma\beta\eta/(1+\beta\eta)$
Ω	$h_{fg}C_r^*/\rho c_p T_r$.

Subscripts

I	variable associated with $z=0$
II	variable associated with $z=L_T$
l	liquid
m	matrix
r	reference
v	vapor
0	variable associated with $z=L_0$
1	variable associated with $z=L_1$.

Superscripts

–	dimensional variable
	parameter evaluated in reference to the condensation region.

ditions which lead to a steady-state solution other than the initial condition. During the transient, the temperature, vapor concentration, and liquid content fields evolve towards a new steady state accompanied by changes in the location and size of the wet zone.

The transport of heat and the species (vapor and liquid) are presently considered to be by diffusion only, and thus convective effects due to condensate motion and air infiltration are not considered. The limitations of this assumption are established in ref. [19]. The conservation equations, using a phenomenological definition of liquid diffusivity D_l, are

$$k_m\frac{\partial^2 T}{\partial z^2}+\Gamma h_{fg}=\rho_m c_m\frac{\partial T}{\partial t} \tag{1}$$

$$D_v\frac{\partial^2 C}{\partial z^2}-\Gamma=\frac{\partial C}{\partial t} \tag{2}$$

$$\rho_l\delta\frac{\partial}{\partial z}\left[D_l(\theta)\frac{\partial\theta}{\partial z}\right]+\Gamma=\rho_l\delta\frac{\partial\theta}{\partial t} \tag{3}$$

subject to the boundary conditions

$$T=T_I,\quad C=C_I,\quad z=0$$
$$T=T_{II},\quad C=C_{II},\quad z=L_T. \tag{4}$$

In the above subscripts m, v, and l denote properties of the medium, vapor, and liquid, respectively, and Γ is the volumetric condensation rate. All other terms are defined in the Nomenclature. In the wet zone the liquid and vapor are in thermodynamic equilibrium and, thus, the vapor is at the saturation concentration (denoted as C^*) corresponding to the local value of temperature: $C(z)=C^*(T(z))$. The liquid content and condensation rate are zero in the dry regions. In the present formulation it is implicitly assumed that the air–vapor mixture is dilute and there are no effects associated with changes in the mixture density across the slab.

The solution of the above equations at steady state requires calculation of the location of the wet zone, and the temperature, vapor concentration and condensate content fields in the porous slab. This problem has been solved in ref. [18], where two spatially steady-state regimes corresponding to mobile and immobile condensates were identified. The non-linear coupling between the conservation equations appear to preclude the analytical solution of the complete unsteady equations. Nevertheless, as the diffusive time-scales controlling the transient behavior of the three T, C, and θ fields are different, for some class of problems,

from the ones controlling the motion of the wet zone boundaries, the two phenomena may be decoupled. It will be shown later that for a large group of system parameters the rate of motion of the wet zone is much slower than the diffusive transients in C, T, and θ fields. Thus, the solution to the present problem is obtained through calculation of quasi-steady fields in time-varying domains.

The approach to the solution of the equations is similar to that of the steady-state conditions given in ref. [18]. The quasi-steady T and θ fields in the wet zone (the C field in the wet zone is uniquely determined by the temperature distribution in that region) are obtained in terms of the (time-varying) positions and temperatures of the wet zone boundaries. By applying energy and mass continuity at the wet zone boundaries the temperature and vapor concentration fields in the wet and dry regions are matched at the wet–dry interfaces, and the temperatures and velocities of the wet zone boundaries are obtained. The resulting equations are numerically integrated in time to obtain the temporal evolution of the system.

The quasi-steady temperature and vapor concentration fields in the wet zone are obtained by combining steady-state forms of equations (1) and (2), and using the Clausius–Clapeyron relationship between saturated vapor and temperature. The (as of yet unknown) wet zone boundary temperatures T_0 and T_1, and positions L_0 and L_1 are used to nondimensionalize the temperature

$$\left(\eta' = \frac{T - \dfrac{T_0+T_1}{2}}{T_0-T_1}\right)$$

and the length scale ($\bar{x} = x/(L_1-L_0)$) in this region. The resulting non-linear differential equation for the temperature field in the wet zone is solved by a perturbation solution technique [18] yielding

$$\eta' = \frac{1}{2}\left[1-\bar{x}-\frac{\exp \lambda'\bar{x}-1}{\exp \lambda'-1}\right]. \tag{5}$$

In the above λ' is the latent heat transport term which denotes the ratio of heat released by condensation of vapor to heat conducted across the wet zone in the absence of condensation. Equation (5) is shown to be accurate for $\lambda' < 6$.

The wet zone boundary temperatures and locations are obtained by matching the temperature and concentration fields in the wet and dry regions. These matching conditions are influenced by the mobility of the condensate. In the solution to the steady-state equations it was shown that two distinct solution regimes exist for the mobile and immobile condensates [18]. In the following the two condensate mobility limits are considered separately.

2.1. *Immobile condensate*

Energy and vapor mass balance for this case at $z = L_0$ are

$$k_m \left.\frac{dT^*}{dz}\right|_{L_0} - k_m \frac{T_0^*-T_1}{L_0} = h_{fg}\rho_l \delta\theta(z=L_0,t)\frac{dL_0}{dt} \tag{6}$$

and

$$D_v \left.\frac{dC^*}{dz}\right|_{L_0} - D_v \frac{C_0^*-C_1}{L_0} = -\rho_l \delta\theta(z=L_0,t)\frac{dL_0}{dt}. \tag{7}$$

Equations (6) and (7) relate the motion of the boundary $z = L_0(t)$ to the balance of energy and diffusion of vapor at that boundary. In the above T^* indicates saturation temperature, thus C^* and T^* are related by the Clausius–Clapeyron relationship. Similar equations may be written at $z = L_1(t)$

$$k_m \left.\frac{dT^*}{dz}\right|_{L_1} - k_m \frac{T_{II}-T_1}{L_T-L_1} = h_{fg}\rho_l \delta\theta(z=L_1,t)\frac{dL_1}{dt} \tag{8}$$

and

$$D_v \left.\frac{dC^*}{dz}\right|_{L_1} - D_v \frac{C_{II}-C_1^*}{L_T-L_1} = -\rho_l \delta\theta(z=L_1,t)\frac{dL_1}{dt}. \tag{9}$$

The liquid content at wet zone boundaries are determined from equation (6) by setting D_l equal to zero

$$\rho_l \delta \frac{\partial\theta}{\partial t} = \Gamma. \tag{10}$$

By combining equations (6) and (7) the dL_0/dt term may be eliminated. Using the Clausius–Clapeyron relationship

$$C^* = C_r^* \exp(\Phi)$$

and the identities

$$\frac{d\bar{z}}{d\bar{x}} = \frac{L_1-L_0}{L_T} \tag{11}$$

$$\frac{d\eta}{d\eta'} = \frac{T_0-T_1}{T_1-T_{II}} \tag{12}$$

the following equation is obtained:

$$\eta_0-\eta_1+\frac{\Omega}{Le\,\beta}[\exp(\Phi_0)-h_l\exp(\Phi_1)] = -\frac{1}{2}\left[1+\frac{\Omega\gamma}{Le}(1+\beta\eta_0)^{-2}\exp(\Phi_0)\right] \times \frac{L_0}{L_1-L_0}\frac{T_0-T_1}{T_1-T_{II}}\left[1+\frac{\lambda'}{\exp\lambda'-1}\right]. \tag{13}$$

In the above η is the temperature variable nondimensionalized by the slab boundary values, Le the Lewis number, and h_l the relative humidity at $z = 0$. All other terms are defined in the Nomenclature.

An equation similar to equation (13) is obtained at

$z = L_1$ by combining equations (8) and (9)

$$\eta_{II} - \eta_1 + \frac{\Omega}{Le\,\beta}[h_{II}\exp(\Phi_{II}) - \exp(\Phi_1)] = -\frac{1}{2}\left[1 + \frac{\Omega\gamma}{Le}(1+\beta\eta_1)^{-2}\exp(\Phi_1)\right] \times \frac{L_T - L_1}{L_1 - L_0}\frac{T_0 - T_1}{T_1 - T_{II}}\left[1 + \frac{\lambda'\exp\lambda'}{\exp\lambda' - 1}\right]. \quad (14)$$

Equations (13) and (14) relate the temperatures at the boundaries of the wet zone (η_0 and η_1) to the location of the wet zone.

By writing the dC^*/dz terms in equations (7) and (9) as

$$\frac{dC^*}{dz} = \frac{dC^*}{dT}\frac{dT^*}{dz}$$

using the dT^*/dz terms from the corresponding energy equations, and the Clausius–Clapeyron equation for dC^*/dT the rates of motion of the wet zone boundaries are obtained in terms of conditions present at the wet–dry interfaces

$$\theta(z = L_1, t)\frac{d(1-\overline{L_1})^2}{d\bar{t}} = 2\left\{[\exp(\Phi_1) - h_{II}\exp(\Phi_{II}) + \gamma\beta(1+\beta\eta_1)^{-2}\exp(\Phi_1)(\eta_{II} - \eta_1)]\Big/\left[1 + \frac{\Omega\gamma}{Le}(1+\beta\eta_1)^{-2}\exp(\Phi_1)\right]\right\} \quad (15)$$

and

$$\theta(z = L_0, t)\frac{d\overline{L_0^2}}{d\bar{t}} = 2\left\{[\exp(\Phi_0) - h_I\exp(\Phi_I) + \gamma\beta(1+\beta\eta_0)^{-2}\exp(\Phi_0)(\eta_I - \eta_0)]\Big/\left[1 + \frac{\Omega\gamma}{Le}(1+\beta\eta_0)^{-2}\exp(\Phi_0)\right]\right\} \quad (16)$$

where

$$\overline{L_0} = \frac{L_0}{L_T}$$

$$\overline{L_1} = \frac{L_1}{L_T}$$

and the non-dimensional time-scale is

$$\bar{t} = \frac{D_v t}{L_T^2}\frac{C_v^*}{\rho_l\delta}. \quad (17)$$

Equations (13)–(16) along with the temperature distribution of equation (5) completely describe the transient motion of the wet zone and the quasi-steady evolution of the three fields. Starting with an initial condition of T, C, and θ fields with a wet zone located somewhere inside the slab, the new location of the wet zone boundaries can be obtained from equations (15) and (16). The new locations are then used to calculate the temperature conditions at the new boundaries of the wet zone and the liquid content is updated. The new values are used for the calculation of the next location of the wet zone. The time integration is continued until a new steady state is reached.

2.2. *Mobile condensate*

The present model of condensate diffusion is based on the postulate that above a critical liquid content (θ_c) the pendular condensate drops coalesce and are driven by surface tension forces from regions of higher liquid content to drier regions. During the transient motion of the wet zone boundaries liquid contents in excess of θ_c lead to the efflux of condensate towards the wet–dry boundaries. At the wet–dry boundaries the condensate effluxes are evaporated, and the liquid content is equal to the non-diffusive component of the condensate θ_c. These conditions modify the boundary mass and energy balance equations of the previous section (equations (6)–(9)) into

at $z = L_0$

$$k_m\frac{dT^*}{dz}\bigg|_{L_0} - k_m\frac{T_0 - T_I}{L_0} = h_{fg}J_0 + h_{fg}\rho_l\delta\theta_c\frac{dL_0}{dt} \quad (18)$$

and

$$D_v\frac{dC^*}{dz}\bigg|_{L_0} - D_v\frac{C_0^* - C_I}{L_0} = -J_0 - \rho_l\delta\theta_c\frac{dL_0}{dt} \quad (19)$$

and at $z = L_1$

$$k_m\frac{dT^*}{dz}\bigg|_{L_1} - k_m\frac{T_{II} - T_1}{L_T - L_1} = -h_{fg}J_1 + h_{fg}\rho_l\delta\theta_c\frac{dL_1}{dt} \quad (20)$$

and

$$D_v\frac{dC^*}{dz}\bigg|_{L_1} - D_v\frac{C_{II} - C_I^*}{L_T - L_1} = J_1 - \rho_l\delta\theta_c\frac{dL_1}{dt}. \quad (21)$$

Similar to the previous section the $dL_{1,0}/dt$ terms can be eliminated by combining energy and mass continuity terms at the boundaries. As the condensate efflux terms cancel out, the equations relating the wet zone boundary temperatures and locations become identical to those obtained for the immobile condensate (equations (13) and (14)), except for the difference in the values of $\theta(z = L_0, L_1)$. The remaining two equations for the rate of motion of the wet zone boundaries are obtained along the lines described in the previous section

$$\theta_c \frac{d(1-\overline{L_1})^2}{d\bar{t}} = 2\left\{[\exp(\Phi_1) - h_{II}\exp(\Phi_{II}) + \gamma\beta(1+\beta\eta_1)^{-2}\exp(\Phi_1)(\eta_{II}-\eta_1)]\Big/\left[1+\frac{\Omega\gamma}{Le}(1+\beta\eta_1)^{-2}\exp(\Phi_1)\right]\right\} - 2\frac{J_1(L_T-L_1)}{D_v C_r^*} \quad (22)$$

and

$$\theta_c \frac{d\overline{L_0^2}}{d\bar{t}} = 2\left\{[\exp(\Phi_0) - h_I\exp(\Phi_I) + \gamma\beta(1+\beta\eta_0)^{-2}\exp(\Phi_0)(\eta_0-\eta_1)]\Big/\left[1+\frac{\Omega\gamma}{Le}(1+\beta\eta_0)^{-2}\exp(\Phi_0)\right]\right\} - 2\frac{J_0 L_0}{D_v C_r^*}. \quad (23)$$

The condensate continuity is given by equation (3) where for mathematical simplicity a mean liquid diffusivity is used

$$\rho_l \delta D_{lm}\frac{\partial^2\theta}{\partial z^2} + \Gamma = \rho_l \delta\frac{\partial\theta}{\partial t}. \quad (24)$$

Equations (13), (14), and (22)–(24) describe the transient motion of the wet zone boundaries in the presence of a mobile condensate.

3. TIME-SCALE ANALYSIS

The time-scale for the motion of the wet zone boundaries are obtained by inspection of equations (15) and (16), for the immobile condensate, and equations (22) and (23) for the mobile condensate.

3.1. *Immobile condensate*

In equations (15) and (16) the terms on the right-hand side are of the order of 1 for water vapor diffusing in air (conditions present in high void fraction open pore porous materials). The time-scale for the motion of the wet–dry boundaries, therefore, are

$$\tau_0 = \frac{L_0^2 \rho_l \delta}{D_v C_r^*}\theta(z = L_0) \quad (25)$$

$$\tau_1 = \frac{(L_T - L_1)^2 \rho_l \delta}{D_v C_r^*}\theta(z = L_1). \quad (26)$$

In order to establish the criterion for the validity of the quasi-steady model, the time-scale for the motion of the boundaries must be compared with the diffusive time-scales. For an immobile condensate, the diffusive time constants are

$$\tau_h = \frac{L_i^2}{\alpha_m}$$

$$\tau_v = \frac{L_i^2}{D_v}$$

$$L_i = (L_0, L_1 - L_0, L_T - L_1). \quad (27)$$

For water vapor diffusing in a high void fraction system Le is of the order of one, and thus, the concentration and heat diffusive time-scales are nearly identical. The ratio of τ_0 and τ_1 to τ_h for various length scale combinations is presented in Table 1. For the motion of the wet zone boundaries to be much slower than the diffusive time constants, the ratios of Table 1 must be much larger than one. This condition indicates that a relationship between the length scales and the liquid content at the wet–dry boundaries must be satisfied. Specifically, for a fixed wet zone size and location the liquid content at the wet–dry boundaries must exceed a minimum value to insure that the rate of motion of the wet zone boundaries is slower than the diffusion of heat and vapor. For a system with similar wet and dry region sizes, the constraint for the validity of the model reduces to a relationship between the local liquid content at the wet–dry boundaries and the ratio of the vapor and condensate densities

$$\delta\theta(z = L_0, L_1) > \frac{C_r^*}{\rho_l}. \quad (28)$$

Table 1. Ratio of diffusive and wet–dry boundary motion time scales

$\frac{\tau_0}{\tau_h}$	$\frac{\delta\rho_l\theta_0}{C_r^*}$	$\left[\frac{L_0}{L_1-L_0}\right]^2\frac{\delta_l\theta_0}{C_r^*}$	$\left[\frac{L_0}{L_T-L_1}\right]^2\frac{\delta_l\theta_0}{C_r^*}$
$\frac{\tau_1}{\tau_h}$	$\left[\frac{L_T-L_1}{L_0}\right]^2\frac{\delta\rho_l\theta_1}{C_r^*}$	$\left[\frac{L_T-L_1}{L_1-L_0}\right]^2\frac{\delta\rho_l\theta_1}{C_r^*}$	$\frac{\delta\rho_l\theta_1}{C_r^*}$
$\frac{\tau_0}{\tau_l}$	$\frac{D_l}{D_v}\frac{\delta\rho_l\theta_c}{C_r^*}$	$\frac{D_l}{D_v}\left[\frac{L_0}{L_1-L_0}\right]^2\frac{\delta\rho_l\theta_c}{C_r^*}$	$\frac{D_l}{D_v}\left[\frac{L_0}{L_T-L_1}\right]^2\frac{\delta\rho_l\theta_c}{C_r^*}$
$\frac{\tau_1}{\tau_l}$	$\frac{D_l}{D_v}\left[\frac{L_T-L_1}{L_0}\right]^2\frac{\delta\rho_l\theta_c}{C_r^*}$	$\frac{D_l}{D_v}\left[\frac{L_T-L_1}{L_1-L_0}\right]^2\frac{\delta\rho_l\theta_c}{C_r^*}$	$\frac{D_l}{D_v}\frac{\delta\rho_l\theta_c}{C_r^*}$

The above implies that for water vapor diffusing in a fiberglass insulation (characterized by δ values close to unity) liquid content at the wet–dry boundaries must be larger than 0.1%.

The ratios of Table 1 indicate that as the sizes of the dry regions or the wet zone decrease the minimum value of $\theta(z = L_0, L_1)$ increases. However, as the value of θ cannot exceed 1, the present results become invalid for vanishingly small wet and dry regions. It must be noted, however, that in cases where either or both of the dry regions are completely absent, for example when a vapor barrier is located on one of the slab boundaries or the slab is entirely wet with vapor barriers on both boundaries of the slab, the above criteria involving the length scales of the non-existing regions do not apply. Under such conditions only the non-zero length scales must be used to establish the validity of the present quasi-steady model.

3.2. *Mobile condensate*

For mobile condensates, the terms in equations (22) and (23) including the liquid flux terms must be evaluated. The steady-state liquid content profile for the case of a mobile condensate in the wet zone is [18]

$$\theta_s(x) = \theta_c + \frac{D_v C_r^*}{D_l \rho_l \delta} \frac{Le\,\beta}{\Omega'} \left[\frac{1}{2} \left(\bar{x} - \frac{\exp \lambda' \bar{x} - 1}{\exp \lambda' - 1} \right) \right] \tag{29}$$

where θ_c is the critical liquid content below which condensate diffusion is absent. Using $J_l = -D_l \partial\theta/\partial x$, the liquid flux terms may be related to other system parameters as

$$\frac{J_0 L_0}{D_v C_r^*} = \frac{Le\,\beta'}{\Omega'} \frac{\exp \lambda' - 1 - \lambda'}{2(\exp \lambda' - 1)} \tag{30}$$

and

$$\frac{J_l (L_1 - L_0)}{D_v C_r^*} = \frac{Le\,\beta'}{\Omega'} \frac{(\lambda' - 1)\exp \lambda' + 1}{2(\exp \lambda' - 1)}. \tag{31}$$

Evaluating the above terms for the transport of moisture in open pore insulations indicates that the liquid flux terms in equations (22) and (23) are of the order of unity. Thus, for the mobile condensate the time-scales for motion of the boundaries are the same as the ones for the immobile condensate, i.e. equations (25) and (26). The diffusive time-scale for condensate diffusion is

$$\tau_l = \frac{(L_1 - L_0)^2}{D_l}. \tag{32}$$

The ratios of wet zone motion to diffusive time-scales for the mobile condensate are similar to those of the immobile condensate with the additional terms relating liquid diffusivity to the rate of motion of the boundaries (τ_0/τ_l and τ_1/τ_l). They are defined in Table 1. Inspection of Table 1 indicates that for the mobile condensate the minimum value of liquid content at the wet–dry boundaries (θ_c) is related to the ratio of liquid and vapor diffusivities, as well as the length scale and vapor–condensate density ratios. The extent of validity of the quasi-steady model both in terms of the minimum value of θ_c and the length scales is, therefore, entirely controlled by the diffusivity of the condensate.

4. CASE STUDY

In the following the methodology developed in this work is applied to the drying of a porous slab for the two regimes of liquid diffusivity. The liquid diffusivity is taken to be equal to the vapor diffusivity so that the quasi-steady requirements are satisfied. The analysis is conducted for high void-fraction fiberglass insulations and, thus, thermophysical properties of air at room temperature are used in the calculations. Other examples such as the effect of vapor barriers on unsteady accumulation of condensate and partial drying of wet slabs are given in ref. [17].

4.1. *Problem statement*

The initial conditions for the transient analysis are obtained from the first spatially steady solution case ($D_l = 0$) study of ref. [18], corresponding to the following slab boundary conditions:

$$T_I = 32°C\ (90°F)$$

$$T_{II} = -4°C\ (25°F)$$

$$h_I = 90\%$$

$$h_{II} = 90\%.$$

The initial liquid content distribution for the immobile condensate case corresponds to a 4000 h long condensation at the above conditions in a 1 ft wide fiberglass slab (Fig. 2). The spatial integral of the initial liquid content for the mobile condensate is equal to

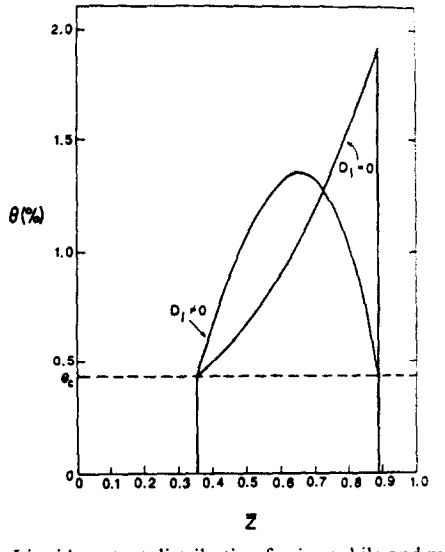

FIG. 2. Liquid content distribution for immobile and mobile condensates

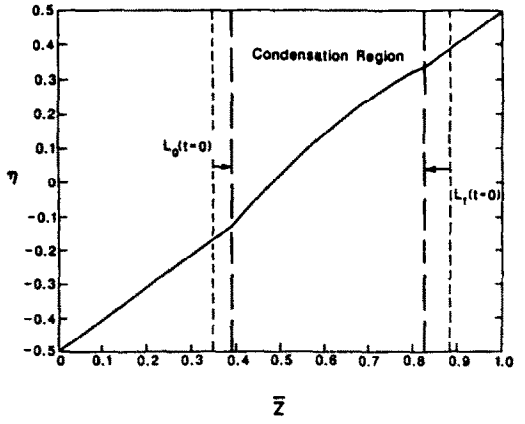

FIG. 3. Non-dimensional temperature profile during transient relocation of the wet zone corresponding to immobile condensate: $D_v t/L_T^2 = 1000$.

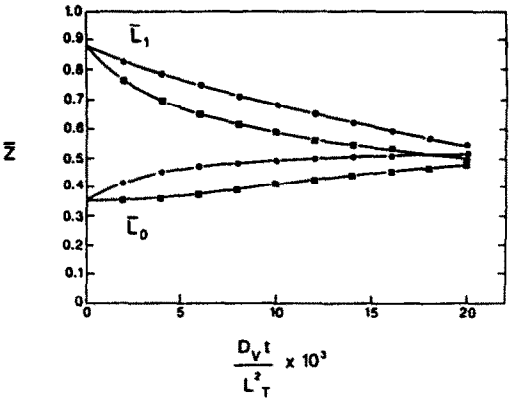

FIG. 5. Evolution of the wet-zone boundaries for mobile (●) and immobile condensates (■).

that of the immobile limit, yet its distribution obeys equation (29).

The transient analysis begins by step changes in the slab boundary conditions from the above to

$$T_I = 16°C\ (60°F)$$

$$T_{II} = 26°C\ (80°F)$$

$$h_I = 80\%$$

$$h_{II} = 85\%.$$

With the new boundary conditions the locations of the hot and cold boundaries of the slab are effectively replaced. The above boundary conditions do not provide for the existence of a wet zone, and, thus, the boundaries of the wet zone evolve towards each other until all the moisture in the slab is evaporated.

4.2. *Results*

The temperature fields in the slab for both regimes of liquid diffusivity at $D_v t/L_T^2 = 1000$ are shown in Figs. 3 and 4, respectively. In both cases the temperature gradients are discontinuous at the wet–dry boundaries reflecting absorption of energy by the evaporating condensate. During the transient motion of the boundaries condensation continuously occurs in the wet zone. However, the magnitude of condensation is negligible in comparison with the initial liquid content. The evolution of the wet zone boundaries is shown in Fig. 5. The difference in the rate of motion of the boundaries for the two types of condensate reflect both the initial liquid content distributions and the condensate mobility. The temperature field in the slab reaches steady state in approximately the same time for both types of condensate, suggesting that the total mass of condensate, as opposed to its mobility, controls the drying period. The analytical solution is carried only up to the stage where the size of the wet zone is sufficiently large for the quasi-steady model to be valid.

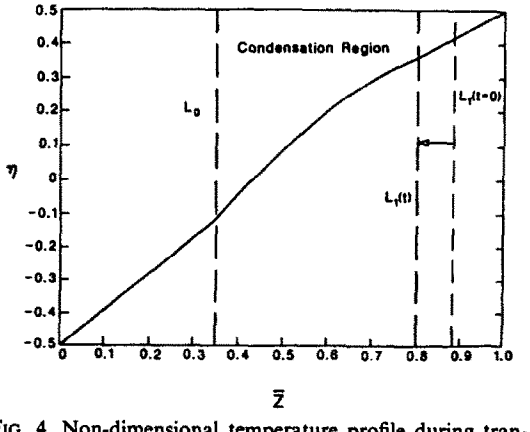

FIG. 4. Non-dimensional temperature profile during transient relocation of the wet zone corresponding to mobile condensate: $D_v t/L_T^2 = 1000$.

5. EXPERIMENTAL RESULTS

In this section the analytical solutions developed in this study are compared with experimental results on heat and mass transfer with phase change in fiberglass insulations.

5.1. *Moisture migration in a porous slab with impermeable boundaries*

Diffusion of heat and mass through a medium density wetted insulation sample has been studied by Thomas *et al.* [16]. The experiment consisted of uniformly wetting six layers of insulation and stacking them together to form a continuous slab. The slab was then heat-sealed in a plastic film. The test section was inserted into a guarded hot plate apparatus and subjected to one-dimensional temperature gradients. The temperature field inside the slab was monitored with thermocouples and the liquid content was measured at regular intervals through disassembly of the slab and measurement of the weight of each of the six layers. The experimental conditions are given in the Appendix.

The analysis of Thomas *et al.*'s data by the present model is obtained by neglecting the presence of the

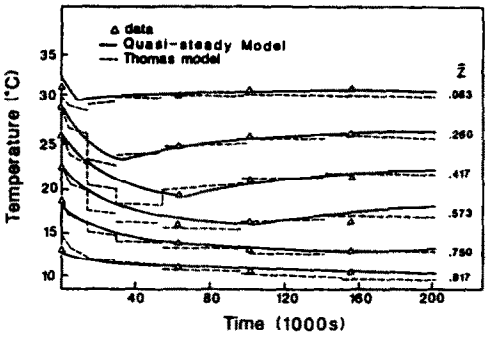

FIG. 6. Comparison of data of ref. [16] with the present model and that of Thomas *et al.* [16].

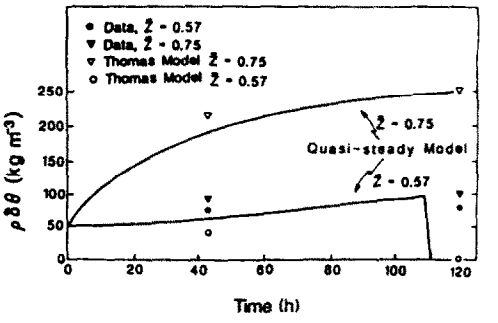

FIG. 8. Moisture distribution change with time. Data of Thomas *et al.* [16], run No. 2.

dry regions and imposing zero mass flux conditions at the slab boundaries. The condensate is assumed to be immobile. The results obtained from the analytical solution of the governing equations are compared with the measured temperature profile in the slab in Fig. 6. The results of the numerical solution of the governing equations by Thomas *et al.* are also presented in Fig. 6. The agreement between both models and the experimental data is extremely good. In Figs. 7 and 8 the calculated transient liquid content fields are compared with two experimental sets of data corresponding to an initial moisture content (dry basis) of 50 and 60%, respectively. The present model appears to predict the liquid content profile more accurately than the numerical model of ref. [13] at low liquid content levels (Fig. 7). Both models, however, appear to mispredict the liquid content profiles at high moisture levels (Fig. 8). This discrepancy may be related to liquid diffusion under gravity and capillary forces at high liquid contents [19].

5.2. *Moisture migration in a porous slab with one vapor barrier*

This experiment was performed by the authors and is reported in ref. [17]. In this experiment a fiberglass test section with a known liquid content distribution was placed inside a Hot–Cold Box, and the cold side of the specimen was covered by a vapor barrier. The Hot–Cold Box consists of two temperature and humidity controlled chambers connected through the specimen. A complete description of the system is given in ref. [17], and the experimental conditions are given in Table 2. The initial measured and modeled liquid content distributions are shown in Fig. 9. In this study liquid water was introduced close to the 'hot' side of the sample, and the boundary conditions were chosen as to provide for the evaporation of the liquid from this region and its recondensation towards the 'cold' impermeable side of the slab. The T, C, and θ fields and the location of the wet zone are calculated by the present model through solution of the governing equations in the wet zone and one dry zone (the region adjacent to the hot side of the slab), and matching of the solutions at that boundary.

The temperature profile in the sample at two different times are shown in Figs. 10 and 11. The present model predicts the location of the wet–dry boundaries (corresponding to the discontinuous change in the temperature gradient) relatively well. Yet, the measured temperature profiles in the wet zone exhibit larger curvatures than the calculated values. The curvature of the temperature profile is related to evaporation–condensation in the wet zone, and is reflected in the value of λ' in equation (5). Thus, the discrepancy between predicted and observed profiles may be related to the values of thermophysical properties used in the calculations, where the effect of water on parameters such as thermal conductivity of the sample are not included. In Fig. 12 the measured final liquid content distribution in the slab is compared with the theoretical predictions. The disagreement between the theoretical and experimental observations may be related to the high value of liquid content at the final stages of the process which could result in liquid

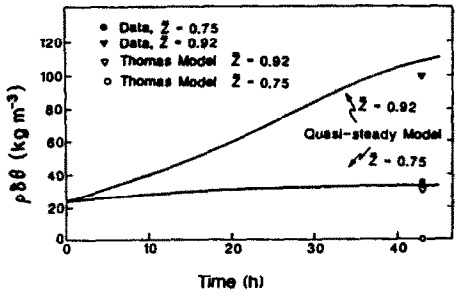

FIG. 7. Moisture distribution change with time. Data of Thomas *et al.* [16], run No. 1.

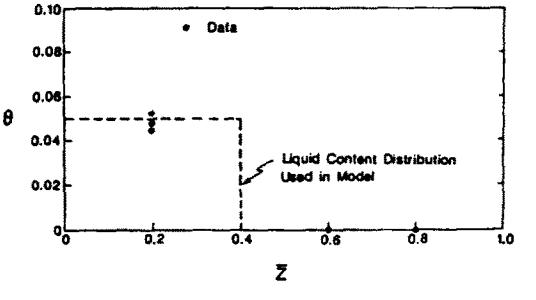

FIG. 9. Initial liquid content distribution in the experiment of Section 5.2.

Table 2. Experimental conditions

Experiment	T_I (°C)	T_{II} (°C)	h_I (%)	h_{II} (%)	Thickness (mm)	Material	Duration (h)
Section 5.1. Vapor barriers on hot and cold sides. Initial condensate content: 0.024 [3]	32	10	†	†	41	medium density fiberglass insulation	50
Section 5.1. Vapor barriers on hot and cold sides. Initial condensate content: 0.051 [3]	31	10	†	†	35	medium density fiberglass insulation	120
Section 5.2. Vapor barriers on cold side. Initial condensate content: Fig. 9	43	17	0.35	†	51	medium density fiberglass insulation	27

† Vapor barrier at this location.

diffusion. Overall, considering that the results of Fig. 12 are obtained after a long time period through which model inaccuracies would accumulate, the agreement between the quasi-steady model and data is encouraging.

6. DISCUSSION

Unsteady simultaneous heat and mass transfer with phase change in an open pore slab is considered and analytical solutions for mobile and immobile condensates are presented. The criteria for the validity of the analytical solutions are presented in terms of time-scales characterizing the diffusive processes and motion of wet–dry boundaries. It is shown that for immobile condensates the obtained solutions are valid up to small liquid contents in the slab. For mobile condensates, on the other hand, the range of validity of the solutions is controlled by the diffusion coefficient of the condensate. The analytical solutions are compared with various experimental results conducted by the authors and others, and reasonable agreements are obtained. The major discrepancy between modelling and experimental results is related to the temperature profile in the wet zone of the slab. It appears that the present model underpredicts the effect of energy release in the wet zone. This discrepancy may be related to three factors. First, the model does not consider changes in the thermophysical properties with moisture content. This

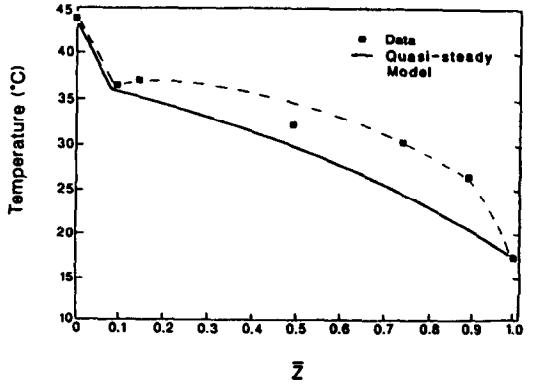

FIG. 10. Temperature profile in the experiment of Section 5.2, time = 23 000 s.

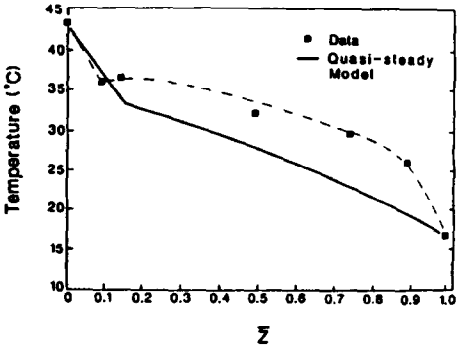

FIG. 11. Temperature profile in the experiment of Section 5.2, time = 100 000 s.

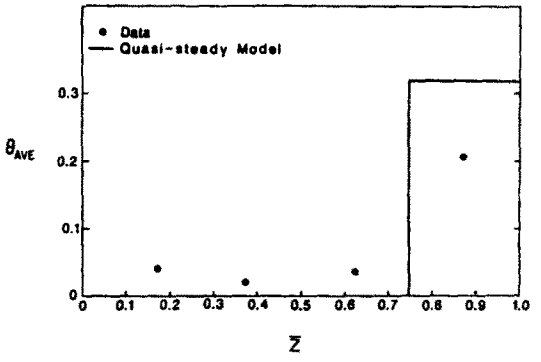

FIG. 12. Final liquid content distribution in the experiment of Section 5.2.

may introduce appreciable errors in high liquid-content regions. Second, inhomogeneities in the fiberglass insulation may lead to spatial variations in the properties of the slab. Third, the assumption of diluteness of the air–vapor mixture may be inaccurate. Of these, the first appears to exert a larger influence on the model predictions. Correction of this model deficiency is not undertaken in this study because there are no reliable relationships between liquid content and properties of fiberglass insulations. As the present solutions involve various thermophysical parameter groups, a rigorous sensitivity analysis of the model predictions and comparison with other experimental data appear to be necessary to identify the required improvements of the model.

Acknowledgement—The authors wish to express their appreciation to Oak Ridge National Laboratory for their financial assistance to this study, and to Prof. L. R. Glicksman for helpful discussions.

REFERENCES

1. N. E. Edlefsen and A. B. C. Anderson, Thermodynamics of soil moisture, *Hilgardia* **15**, 31–298 (1943).
2. D. A. deVries, Simultaneous transfer of heat and moisture in porous media, *Trans. Am. Geophys.* **39**, 909–916 (1958).
3. J. W. Cary and S. A. Taylor, The interaction of the simultaneous diffusion of heat and water vapor, *Soil Sci. Proc.* 413–416 (1962).
4. A. V. Luikov, *Heat and Mass Transfer in Capillary Porous Bodies*. Pergamon Press, Oxford (1966).
5. H. A. Dinulescu and E. R. G. Eckert, Analysis of the one-dimensional moisture migration caused by temperature gradients in a porous medium, *Int. J. Heat Mass Transfer* **23**, 1069–1078 (1980).
6. E. R. G. Eckert and M. Faghri, A general analysis of moisture migration caused by temperature differences in an unsaturated porous medium, *Int. J. Heat Mass Transfer* **23**, 1613–1623 (1980).
7. C. L. D. Huang, Multi-phase moisture transfer in porous media subjected to temperature gradients, *Int. J. Heat Mass Transfer* **22**, 1295–1307 (1979).
8. Y. Ogniewicz and C. L. Tien, Analysis of condensation in porous insulation, *Int. J. Heat Mass Transfer* **24**, 421–429 (1981).
9. K. Vafai and S. Sarkar, Condensation effects in fibrous insulation slabs, *J. Heat Transfer* **108**, 667–675 (1986).
10. K. Vafai and S. Whitaker, Heat and mass transfer accompanied with phase change in porous insulations, *J. Heat Transfer* **108**, 132–140 (1980).
11. P. Marsh, *Thermal Insulation and Condensation*. The Construction Press, London (1979).
12. M. Bomberg, Moisture flow through porous building materials, Lund Institute of Technology, Lund, Sweden (December 1973).
13. R. P. Tye and S. C. Spinney, A study of the effects of moisture vapor on thermal transmittance characteristics of cellulose fiber thermal insulation, *J. Thermal Insulation* **2**, 175–196 (1979).
14. M. B. Stewart, An experimental approach to the study of moisture dynamics in walls, ASTM STP 779, 92–101 (1982).
15. C. Langlais, M. Hyrien and S. Karlsfeld, Moisture migration in fibrous insulating material under the influence of a thermal gradient, Moisture Migration in Buildings, ASTM STP 779, 191–206 (1982).
16. W. C. Thomas, G. P. Bal and R. J. Onega, Heat and moisture transfer in a glass roof-insulating material, ASTM STP 789, 582–601 (1983).
17. A. P. Shapiro, Steady and unsteady heat and mass transfer through porous media with phase change, S. M. Thesis, M.I.T., Cambridge, Massachusetts (1987).
18. S. Motakef and M. A. El-Masri, Simultaneous heat and mass transfer with phase change in a porous slab, *Int. J. Heat Mass Transfer* **29**, 1503–1512 (1986).
19. S. Motakef, Simultaneous heat and mass transport with phase change in insulated structures, Ph.D. Thesis, M.I.T., Cambridge, Massachusetts (1984).

TRANSFERT VARIABLE DE CHALEUR ET DE MASSE AVEC CHANGEMENT DE PHASE DANS DES PLAQUES POREUSES: SOLUTION ANALYTIQUES ET RESULTATS EXPERIMENTAUX

Résumé—On étudie analytiquement le transfert variable de chaleur et de masse monodimensionnel avec changement de phase dans une plaque poreuse. On montre que pour une grande classe de problèmes, la vitesse de déplacement de la zone sèche peut être découplée du changement des champs de température et d'espèces, et le mécanisme peut être réduit à celui de champs quasi-statiques dans des domaines dépendants du temps. Des résultats analytiques sont présentés pour des condensats mobiles et immobiles. Un accord raisonnable est obtenu entre les solution analytiques et les données expérimentales.

INSTATIONÄRER WÄRME- UND STOFFTRANSPORT MIT PHASENWECHSEL IN PORÖSEN SCHICHTEN—ANALYTISCHE LÖSUNGEN UND EXPERIMENTELLE ERGEBNISSE

Zusammenfassung—In einer porösen Schicht wird der instationäre eindimensionale Wärme- und Stofftransport mit Phasenwechsel analytisch untersucht. Es zeigt sich, daß für viele Probleme die Bewegungsgeschwindigkeiten der feuchten Zone von den zeitlichen Veränderungen der Temperatur- und Konzentrationsverteilung abgekoppelt werden kann. Der instationäre Prozeß kann dadurch auf quasistationäre Felder in zeitlich variablen Bereichen reduziert werden. Für bewegliches und unbewegliches Kondensat werden analytische Ergebnisse vorgestellt; die Übereinstimmung mit experimentellen Daten ist zufriedenstellend.

НЕСТАЦИОНАРНЫЙ ТЕПЛО- И МАССОПЕРЕНОС С ФАЗОВЫМ ПЕРЕХОДОМ В ПОРИСТЫХ СЛИТКАХ: АНАЛИТИЧЕСКИЕ РЕШЕНИЯ И ЭКСПЕРИМЕНТАЛЬНЫЕ РЕЗУЛЬТАТЫ

Аннотация—Аналитически исследуется нестационарный одномерный тепло- и массоперенос с фазовым переходом в пористом слитке. Показано, что для большого класса задач скорость перемещения влажной зоны может быть независима от нестационарного изменения полей температуры и образцов, а переходный процесс может быть сведен к квазистационарным полям в зависящих от времени областях. Представлены аналитические результаты для подвижных и неподвижных конденсатов. Аналитические решения удовлетворительно согласуются с экспериментальными данными.